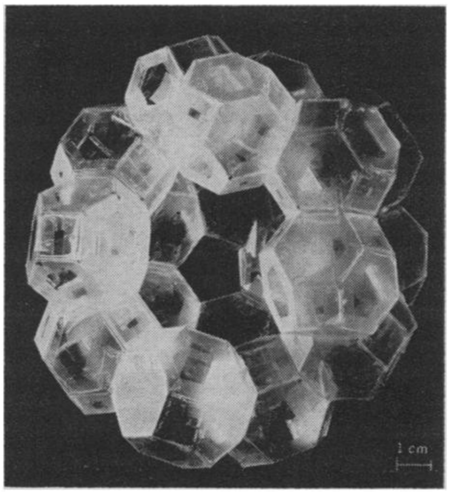

Fig. 3. Model of basket-shaped crystals.

sodium chloride is that of ferrocyanide salts. Concentrations as low as 10 parts per million cause the formation of vicinal (110) faces on (100) planes, thus preventing strongly bonding salt bridges from forming between contiguous crystals. (This is the basis for the anti-caking patents.) At higher concentrations growth layers on (100) are suppressed, and the 12 edges extend themselves around concave cube faces to form skeletal cubes. At still higher concentrations edge growth, as well, is suppressed and the eight corners extend, forming spiky star-like crystals. This last effect forms the basis of the patents on sodium chloride of low-bulk density.

On moist salt crystals drying in air, ferrocyanide salts at very high concentrations cause dendritic growth (Fig. 1). These dendrites are cryptocrystalline extensions of cube corners and grow to lengths of 2.5 cm or more.

Seven effective habit-modifying agents reported here are cysteine, creatinine, papain, monosodium glutamate, sodium hexametaphosphate, a combination of sodium hexametaphosphate and an aluminum salt, and aluminon. The first five agents cause the formation of octahedra. Aluminon causes the formation of very finely divided octahedra, and if there is contamination by an aluminum salt the crystals are colored pink.

The most interesting modifier of crystal habit was the combination of sodium hexametaphosphate with a soluble aluminum salt. When a soluble aluminum salt was present in the system the formation of octahedra resulting from the action of sodium hexametaphosphate was suppressed and cubic crystals formed. However, the two agents in proper ratio in the vacuum evaporator yield in quantity coarse crystal aggregates of sodium chloride shaped like baskets (Fig. 2).

These bulky basket-shaped crystals are aggregates of a geometric solid described by Kelvin (*8*) as regular tetrakaidecahedra. This 14-faced combination is a cubo-octahedron with eight hexagonal (111) faces and six square (100) faces. All edges are equal in length. The aggregate structure is probably derived by accretions of tetrakaidecahedra as in twin position. When in this position the joined (111) faces have a common edge (110) and the adjacent (100) faces have a common edge (001). A model was made with this orientation of the units and a striking similarity to the actual crystal aggregate was found (Fig. 3).

The possibility exists that since (111) faces consist of lattice planes containing, at any given instant, all sodium or all chlorine atoms and other lattice planes alternate sodium-chlorine-sodium, the attractive forces between (111) faces are greater than those between (100) faces. That crystal growth by accretion on similar parallel planes is probable was shown by Schubnikov (*5*, p. 247).

The combination of microscope screening and vacuum evaporation has been found to be a useful technique in this specific application. It would seem to be useful in other crystal-growing processes either to select agents for use in growing better crystals or even to determine contaminants causing poor crystallization.

RICHARD S. PLOSS
Baird-Atomic, Inc., 33 University Road, Cambridge, Massachusetts

References and Notes

1. I thank International Salt Company, Clarks Summit, Pa. for supporting this research and for permission to publish.
2. I thank Professor P. Kerr of Columbia University and Professor E. Sargent of Long Island University for opening their reagent shelves to me.
3. O. Lehmann, *Molekularphysik* 1 (1888).
4. C. Frondel, *Am. Mineralogist* **25**, 103 (1940).
5. H. E. Buckley, *Crystal Growth* (Wiley, New York, ed. 2, 1952), pp. 247, 556.
6. U.S. patent 2,642,335, 16 June 1953, assigned by May and Scott to ICI; U.S. patent 3,-090,756, 21 May 1963, assigned by Dale W. Kaufmann to International Salt Company.
7. D. W. Kaufmann, *Sodium Chloride* (Reinhold, New York, 1960), p. 15.
8. W. Thompson (Lord Kelvin), *Phil. Mag.* **24**, 503 (1887).

17 January 1964

Origin of Oceanic Manganese Minerals

Abstract. *A criterion is suggested for discrimination between ferromanganese oxide minerals, deposited after the introduction of manganese and associated elements in sea water solution at submarine vulcanism, and minerals which are slowly formed from dilute solution, largely of continental origin. The simultaneous injection of thorium into the ocean by submarine vulcanism is indicated, and its differentiation from continental thorium introduced into the ocean by runoff is discussed.*

Since the discovery of the widespread occurrence of manganese oxide nodules on the ocean floor by Murray and his collaborators (*1*) the origin of these aggregates has been extensively debated. Some authors have assumed submarine vulcanism as the main source of the manganese; others have pointed at the depletion of manganese in continental and epicontinental sediments, leading to a net transport of manganese to the ocean floor. This discussion has recently been summarized and implemented by Bonatti and Nayudu (*2*). A review of the present knowledge of the structure and composition of the aggregates has been given by Arrhenius (*3*).

Bonatti and Nayudu (*2*) have stressed the extensive direct and circumstantial evidence for volcanic origin of the main constituents. However, it also appears beyond doubt that a net transport of manganese takes place from the continental shelves into the deep ocean (*4*). Consequently one is led to assume that both of these processes contribute to the accretion of manganese oxide minerals on the ocean floor (*5*). It is interesting under these circumstances to attempt a discrimination between manganese oxides derived from submarine eruptives, on one hand, and oxide minerals composed essentially of manganese derived from weathering on the continents, on the other. Numerous chemical analyses carried out on manganese nodules, primarily from the Pacific Ocean (*5, 6*) are available as a basis for such an attempt.

It appears evident from observation of glass specimens, which have reacted with sea water, that considerable amounts of ions of the transition elements in their lower oxidation states may be released into solution in sea water at submarine volcanic effusions. Many of these species, including iron and manganese, are unstable at the oxygen content of normal sea water and would be expected to be successively precipitated near the site of eruption or other hydrothermal activity. A detailed discussion of these reactions is given by Boström (*7*). Dissolved manganese transported from the continent, as well as manganese remaining in solution after oxidation and hydrolysis of the bulk of the volcanic effusive release, would have to prevail in extremely dilute solution, presumably in the form of some uncharged hydroxide species (*8*). The amount of manganese in sea water passing through filter mesh of 0.5 μm has been measured by Goldberg (*9*), and the order of concentration found, 4×10^{-8} mole/liter, constitutes the best estimate of the amount in solution. As indicated by Boström (*7*), the most important factor controlling the rate of oxidation after a volcanic effusion on the deep ocean floor is the advection of dissolved oxygen; since its normal concentration in sea water is low (1.3×10^{-4} mole/liter can be taken as a representative figure), the equivalent of about 4000 liters of sea water would be needed for the oxidation of one mole of divalent manganese into quadrivalent form. Buser and Grütter (*10*) have demonstrated that the solid phase which forms at the initially low oxidation potential is a (probably metastable) mixed layer structure consisting of alternating sheets of MnO_2 and $Mn(OH)_2$. The structure is strongly disordered; as a result the steric requirements on substituting ions are not particularly stringent, and large amounts of metal ions of widely varying size and ligand-field characteristics are incorporated at the presumably rapid precipitation from volcanogenic solutions.

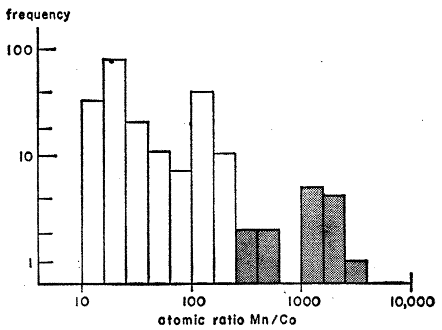

Fig. 1. Frequency distribution of the ratio Mn/Co in manganese nodules from the Pacific Ocean floor. The collective has been divided into a high and a low cobalt group by an arbitrary limit at the atomic ratio Mn/Co = 300.

Single-sheet structures of MnO_2 constitute the stable phase at a high redox potential—that is, in the late stages of the oxidation process when the concentrations of reacting metal cations are low in comparison with the concentration of dissolved oxygen. Such high ratios of oxygen to reactive-cation concentration would be expected to prevail at the precipitation of manganese species which have been diluted during a long residence in solution, or of such species which have been originally introduced in the ocean in a highly diluted state (continental runoff) including the dissolved manganese from the continents. The resultant, highly oxidized MnO_2 phase types found on the ocean floor generally display a relatively high degree of ordering of the constituent molecular sheets in contrast to the Mn(II)-Mn(IV) mixed layer structures. The indiscriminate incorporation of a broad assemblage of foreign ions, which is typical of these rapidly precipitated, disordered structures with mixed ionic charge, is absent in the well ordered aggregates of MnO_2 and FeOOH, presumably slowly crystallized. This slow growth has most likely taken place from solution. The possibility can not be excluded, however, that secondary oxidation and recrystallization of the mixed-layer structure can take place over a long time, and it does for this reason appear safer at the present time to base a diagnosis of the origin and mode of deposition not solely on the crystal structure of the mineral. Other cations, accepted in the Mn(II) layers of the mixed structure but not fitting in the MnO_2 crystal could, however, furnish a memory of the original redox conditions at the time of deposition. Among the 3*d*-elements cobalt would be expected to be the most advantageous tracer of this kind; chromium, iron, nickel, and copper are less suitable, owing to their abundance relations, the nature of the dissolved species, and their behavior in igneous systems. A more detailed discussion of these limiting conditions is given by Arrhenius and Bonatti (*11*). Cobalt probably prevails in divalent form in the sea water and remains stable at a potential where Mn(II) is oxidized (*8; 11,* Fig. 1; *12*). The Co(II) can be expected to enter in substitution for Mn(II) in the mixed-layer minerals which indicate a low redox potential at the time of formation. Large amounts of cobalt in the manganese oxide phase are indeed found in nodules with a high total content of cobalt (*11*) (Table 1).

Table 1. Thorium and cobalt content of the total aggregate of manganese nodules from various locations. The composition of the different phases constituting these aggregates is discussed by Arrhenius (*3*, Table 2) and by Arrhenius and Bonatti (*11*).

Sample		Th* (ppm)	Co† (ppm)
Latitude	Longitude		
	Dwd BD4		
17°20′S	146°30′W	84	9100
	Dwd HD72		
25°31′S	85°14′W	58	4400
	Alb 4713		
9°57′N	137°47′W	75	1100
	Alb 4711		
7°48′S	94°06′W	17	295
	Alb 4721		
8°08′S	104°11′W	5	520
	Alb 2		
28°23′N	126°57′W	9	60

* Colorimetric determination after separation by anion exchange (*17*). † Optical spectrometric determination (by A. Chodos and E. Godijn) on an aliquot of the sample used for thorium analysis.

Conversely, a lack of cobalt and divalent manganese in the mineral structure of manganese oxide would indicate a high oxidation state of the manganese at the time of precipitation, presumably associated with slow deposition from highly dilute solution with

Table 2. Thorium in replacement minerals on marine skeletal apatite and in phosphatized plant tissue as compared to the average in igneous rocks.

Sample	Th (ppm)
Fish debris from pelagic sediments, N, Equatorial Pacific* †	92
Fish debris from pelagic sediment, off Mexico	73
Fish debris from pelagic sediment, N, Equatorial Pacific*	30
Fish debris from pelagic sediment, Modelo formation, Calif. (Tertiary) (Comparatively rapidly accumulating shallow water sediment)* †	24
Shark's tooth, Mesozoic, Colorado	847
Phosphatized bark, Middle American Trench†	225
Igneous rocks, average (*18*)	12

* The significance of the distribution of rare earth elements in these samples is discussed by Arrhenius and Bonatti (*11*, Fig. 4 and text). † The composition of these samples, particularly the significance of their uranium content, is discussed by Arrhenius (*3*, Table 5 and text).

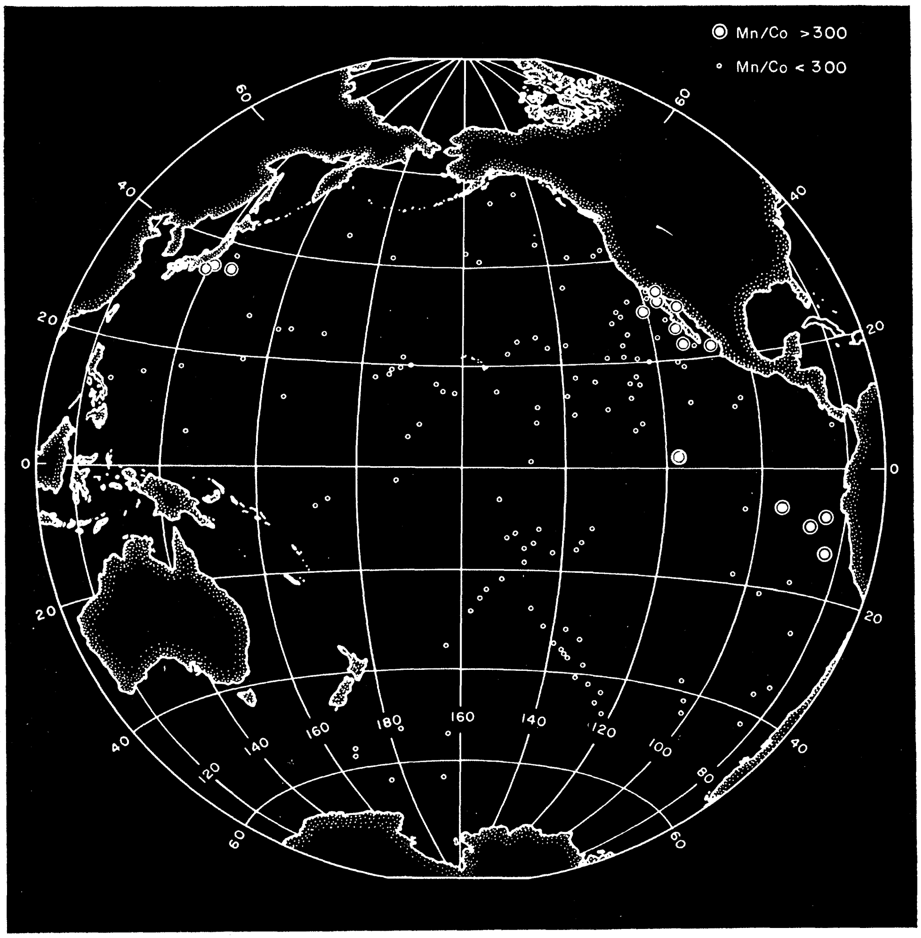

Fig. 2. Geographic distribution of the atomic ratio Mn/Co in Pacific manganese nodules. Small, unfilled circles indicate the location of nodules with a high content of cobalt (Mn/Co less than 300); large, filled circles correspond to cobalt deficient concretions with more than 300 atoms of manganese per atom of cobalt. The cobalt deficient concretions appear to have crystallized slowly from dilute solution of manganese. Structure, composition, and association with decomposed volcanics indicate that the nodules with a high cobalt content formed by a process of rapid precipitation from vulcanogenic sea water solution, partially depleted in oxygen.

normal oxygen content as already outlined. Perturbations of this distribution process by regional variation of the cobalt content of the source rock is minimized by the relatively even partition of cobalt between acid and basic rocks, in contrast to most other 3*d*-elements.

Under these circumstances it is of interest to establish the frequency and areal distributions of cobalt in manganese oxide minerals. A significant number of widely distributed analyses exists only for the Pacific Ocean. Figure 1 shows the frequency distribution of the atomic ratio of Mn to Co in a collective of ferromanganese concretions from the Pacific. An arbitrary limit between high and low ratios has been drawn in the frequency distribution at the ratio 300 atoms of Mn per atom of Co. Figure 2 shows the areal distribution of high and low ratios. With the exception of an equatorial specimen, the high Mn to Co ratios are distributed in the marginal areas of the ocean. One is consequently led to believe that the majority of the manganese nodules found in the central parts of the Pacific basin are rapidly precipitated from short-lived solutions of divalent manganese ion transferred into the ocean mainly by submarine vulcanism. It is further suggested that the major part of the manganese, derived from continental weathering, is precipitated in a tetravalent state in the vicinity of the continents.

An empirical observation of considerable radiochemical interest is the concentration of thorium in those ferromanganese concretions which are believed to be of volcanic origin, and the paucity of this element in those oxide mineral deposits which are thought to be of dominantly continental origin (Table 1). This distribution indicates that thorium and, from other evidence (*13*), also uranium, are contributed to the ocean partly from submarine eruptives. The major part of the volcanically contributed thorium is concentrated into the primary zeolites (harmotome) forming in the early stages of interaction between the lava and sea water (*3*, Fig. 28*b*; *14*). However, a considerable fraction of the thorium apparently escapes immediate precipitation and becomes incorporated primarily in the iron—and to a smaller extent in the manganese oxide minerals formed at the gradual advection of oxygen to the vulcanogenic reactive solution (*3*, Table 2). This mobility of thorium can be understood in terms of the hydrolysis mechanism established by Hietanen (*15*) involving a gradual polymerization of Th(O,OH)Th links into chainlike ion complexes with decreasing solubility as the number of links increases.

As is evident from Table 1, thorium is, like cobalt, largely excluded from the slowly precipitating iron hydroxide and manganese oxide structures. The thorium species, brought into solution in the ocean from weathering continental rocks, would consequently be expected to be found in other slowly growing crystalline phases with a favorable structure for the accommodation of this element. Probably the most important crystals with this function are the rare-earth phosphates which form authigenic overgrowths on dissolving microcrystalline apatite on the ocean floor (*3*, *11*, *16*), and which invariably are found to have accumulated large amounts of thorium (Table 2).

G. ARRHENIUS
J. MERO *
J. KORKISCH

Scripps Institution of Oceanography,
University of California, La Jolla,
Department of Mineral Technology,
University of California, Berkeley
Institute of Chemistry,
University of Vienna, Vienna, Austria

References and Notes

1. J. Murray and A. F. Renard, *Deep-Sea Deposits: Report of Challenger Expedition*, (London, 1891).
2. E. Bonatti and Y. R. Nayudu, in preparation.
3. G. Arrhenius, in *The Sea*, M. Hill, Ed. (Interscience, New York, 1963), vol. 3, p. 663.
4. E. D. Goldberg and G. Arrhenius, *Geochem. Cosmochim. Acta* **13**, 153 (1958); P. H. Kuenen, *Marine Geology* (Wiley, New York, 1950).

5. N. S. Skorniakova, P. F. Andrushenko, L. S. Fomina, *Okeanologiya* **2**, 264 (1962).
6. J. L. Mero, *Econ. Geol.* **57**, 747 (1962); *The Mineral Resources of the Sea* (Elsevier, Amsterdam, in press).
7. K. Boström, *Geochemical Aspects of Submarine Vulcanism* (in preparation).
8. L. G. Sillén, "The physical chemistry of sea water," in *Oceangraphy*, M. Sears, Ed. (AAAS, Publ. 67, Washington, 1961)..
9. E. D. Goldberg, *J. Chem. Educ.* **35**, 116 (1958).
10. W. Buser and A. Grütter, *Schweiz. Mineral Petrog. Mitt.* **36**, 49 (1956).
11. G. Arrhenius and E. Bonatti, "Neptunism and vulcanism in the ocean," in *Progress in Oceanography* (Pettersson Volume), F. Koczy and M. Sears, Eds. (Pergamon, New York, 1964).
12. E. D. Goldberg, "Chemistry in the oceans," in *Oceanography*, M. Sears, Ed. (AAAS, Publ. 67, Washington, 1961).
13. G. Arrhenius and associates, paper in preparation.
14. E. Picciotto, "Radioactive elements and deep sea sediments," in *Oceanography*, M. Sears, Ed. (AAAS, Publ. 67, Washington, 1961).
15. S. Hietanen, *Acta Chem. Scand.* **8**, 1626 (1954).
16. G. Arrhenius, M. Bramlette, E. Picciotto, *Nature* **180**, 85 (1957).
17. J. Korkisch and G. Arrhenius, *Anal. Chem.*, in press.
18. V. M. Goldschmidt, *Geochemistry* (Clarendon Press, Oxford, 1954).

19. Supported by U.S. Atomic Energy Commission grant [AT (11-1-34] and an award from the American Chemical Society's Petroleum Research Fund (875-C6). We thank Dr. K. Boström for valuable discussion. Contribution from the Scripps Institution of Oceanography, New Series.

* Present address: Newport News Shipbuilding and Drydock Co., Newport News, Va.

24 January 1964 ■

X-Ray-Induced Bulk Photovoltaic Effect in Insulators

Abstract. *When an insulator, sandwiched between metals of dissimilar work functions, is irradiated with x-radiation, a voltage related to the contact potential difference of the metals is observed. This phenomenon, known as the bulk photovoltaic effect, has been demonstrated in a variety of metal-insulator-metal combinations. Evidence that the voltage is not generated by junctions, barrier layers, or similar other phenomena is presented.*

The bulk photovoltaic effect in insulators, previously described theoretically by Tauc (*1*), has heretofore been demonstrated experimentally only with visible and ultraviolet light (*2*).

One type of cell which displays the bulk photovoltaic effect consists of an insulator between, and in intimate contact with, two metals of different work functions. The contact potential difference between these metals appears as a voltage across the insulator when the metals are connected through an external resistance. The resulting electric field in the insulator will accelerate any current carriers raised into the conduction band. We have studied cells in which the energy needed to excite current carriers is provided by ionizing radiation—50 kv (peak) x-rays—absorbed in the insulator. In this case, part of the energy lost by radiation in the insulator is delivered to carriers raised to the conduction band and is thus made available to do work in an external circuit. This effect is fundamentally different from the better known "barrier-layer photovoltaic effect" which is observed only in true semiconductors and depends for its voltage upon a depletion region due to a *p-n* junction. (See *1* for a discussion of the distinction between these two phenomena.)

Cells which display the bulk photovoltaic effect under the beam from a 50-kv x-ray tube have been fabricated from a variety of insulators in different thicknesses and with different pairs of electrode metals. The combinations in which we have observed the effect are listed in Table 1.

The cells enumerated in Table 1 gave open-circuit (10^{11} ohm electrometer load) voltages ranging from 0.15 for the CdS (with In, Au) up to 1.85 for the anodized Al_2O_3 between Al, Au. The insulator thicknesses much greater than 10^{-4} cm gave short-circuit currents which were orders of magnitude lower than the thinner insulators made by anodizing, as might be expected owing to carrier recombination and trapping. By far the highest output was obtained from the thickest achievable Ta:anodized Ta_2O_5:Au cells, which gave up to 5 μa short-circuit current when irradiated with 50-kv x-rays (tube current was 44 ma). The response of typical Ta:anodized Ta_2O_5:Au cells is shown in Fig. 1. Of particular interest are the open-circuit voltages (the highest value of voltage) and the short-circuit currents (at the intersection with the horizontal axis).

Two "null" cells were fabricated to demonstrate that the voltage observed was not generated by junctions or some other phenomenon within the insulator. (i) A cell of Al:anodized Al_2O_3:Al was prepared on the same anodized Al block as a cell of Al:anodized Al_2O_3:Au. Under x-irradiation this Al:Al cell gave an open-circuit voltage of less than 0.050 compared to 1.85 for the Al:Au cell on the same oxide layer. (ii) A cell of Ta:anodized Ta_2O_5:Al was prepared which gave an open-circuit voltage of only 0.2 compared to all other Ta: anodized Ta_2O_5 cells using either Au or Ag, which gave voltages in excess of 0.95. Since the work function difference of Ta:Al is about 0.1 volt (much lower than the Ta:Au or Ta:Ag differences which approach 1 volt), this qualitatively constitutes a null experiment.

These null cells demonstrate that the cell voltage depends on the existence of a large contact potential difference between the electrode metals.

To demonstrate that the phenomenon is not due to a depletion region (barrier) near one electrode, cells of Ta: anodized Ta_2O_5:Au were prepared with the oxide layers of different thicknesses ranging from 0.1 to 3.5 μ. The short-circuit photocurrents from cells with oxide 2.2 and 3.5 μ thick (thickness measured by metallurgical sectioning) were directly proportional to the oxide thickness, thus showing that carrier collection is a bulk effect.

Some of the cells which gave high output under the x-ray beam were ex-

Table 1. Metal-insulator-metal combinations in which the x-ray induced bulk photovoltaic effect has been demonstrated. The first-named electrode metal is a substrate upon which the insulator was deposited; the last (more noble) metal was evaporated in vacuum (except for the Al: sulfur: Pt cell).

Insulator	Insulator thickness (cm)
Al,Au electrode	
Al_2O_3 (anodized)	10^{-5}, 3×10^{-5}
Al_2O_3 (sapphire)	3×10^{-2}
$CdWO_4$ (crystal)	7×10^{-2}
$CaWo_4$ (crystal)	3×10^{-2}
Mylar film	10^{-3}, 3×10^{-3}
Ta,Au electrode	
Ta_2O_5 (anodized)	10^{-5} to 10^{-4}
Silicone varnish	$\sim 10^{-3}$
Ta,Ag electrode	
Ta_2O_5 (anodized)	7×10^{-5}
Al,Pt electrode	
Sulfur (cast)	1.5×10^{-2}
In,Au electrode	
CdS (10^{12} ohm-cm crystal)	8×10^{-3}
Ta,Al electrode	
Ta_2O_5 (anodized)	7×10^{-5}
Ta,Pt electrode	
Ta_2O_5 (anodized)	10^{-4}